

Preserving cell shape under environmental stress

Boaz Cook¹, Robert W. Hardy¹, William B. McConnaughey² & Charles S. Zuker¹

Maintaining cell shape and tone is crucial for the function and survival of cells and tissues. Mechanotransduction relies on the transformation of minuscule mechanical forces into high-fidelity electrical responses^{1–3}. When mechanoreceptors are stimulated, mechanically sensitive cation channels open and produce an inward transduction current that depolarizes the cell. For this process to operate effectively, the transduction machinery has to retain integrity and remain unfailingly independent of environmental changes. This is particularly challenging for poikilothermic organisms, where changes in temperature in the environment may impact the function of mechanoreceptor neurons. Thus, we wondered how insects whose habitat might quickly vary over several tens of degrees of temperature manage to maintain highly effective mechanical senses. We screened for *Drosophila* mutants with defective mechanical responses at elevated ambient temperatures, and identified a gene, *spam*, whose role is to protect the mechanosensory organ from massive cellular deformation caused by heat-induced osmotic imbalance. Here we show that Spam protein forms an extracellular shield that guards mechanosensory neurons from environmental insult. Remarkably, heterologously expressed Spam protein also endowed other cells with superb defence against physically and chemically induced deformation. We studied the mechanical impact of Spam coating and show that spam-coated cells are up to ten times stiffer than uncoated controls. Together, these results help explain how poikilothermic organisms preserve the architecture of critical cells during environmental stress, and illustrate an elegant and simple solution to such challenge.

Fly mechanoreceptor neurons (MRNs) are essential for several critical functions such as hearing, proprioception, flight control and touch sensing. Their mis-function leads to uncoordination and loss of mechanoreceptor responses^{4,5}. To identify components of the machinery that preserve the functional integrity of the mechanosensory apparatus at high environmental temperatures, we performed a genetic screen for temperature-sensitive uncoordinated flies; we anticipated that loss-of-function mutations in such components may render MRN function highly susceptible to the elevated temperature. Approximately 12,000 ethylmethane-sulphonate-mutagenized homozygous lines⁶ were examined for intact locomotor responses at room temperature, but defective behaviour after 1 h at 37 °C. One mutant line, 2649, had no apparent defects at room temperature, including walking, feeding and flying. However, upon shifting to the restrictive temperature, the flies gradually lost the ability to fly, to stand upside down and to climb walls, until eventually they could only lie and sporadically move their legs, wings and mouthparts in an uncoordinated manner (Supplementary Fig. 1 and Supplementary videos). Genetic mapping and transformation rescue experiments proved that the mechanosensory defects of line 2649 are due to a non-sense mutation in the spacemaker gene (*spam*; see Fig. 1).

Recently, we showed that *spam* encodes an extracellular protein required for creating the intra-rhabdomeral space in the compound eyes of insects with open rhabdom systems⁷. There, Spam provides

the extracellular substrate to sustain the precise arrangement of rhabdomeres within each ommatidium⁷. Notably, the other sites of Spam expression are on mechanosensory and chemosensory neurons⁸. To

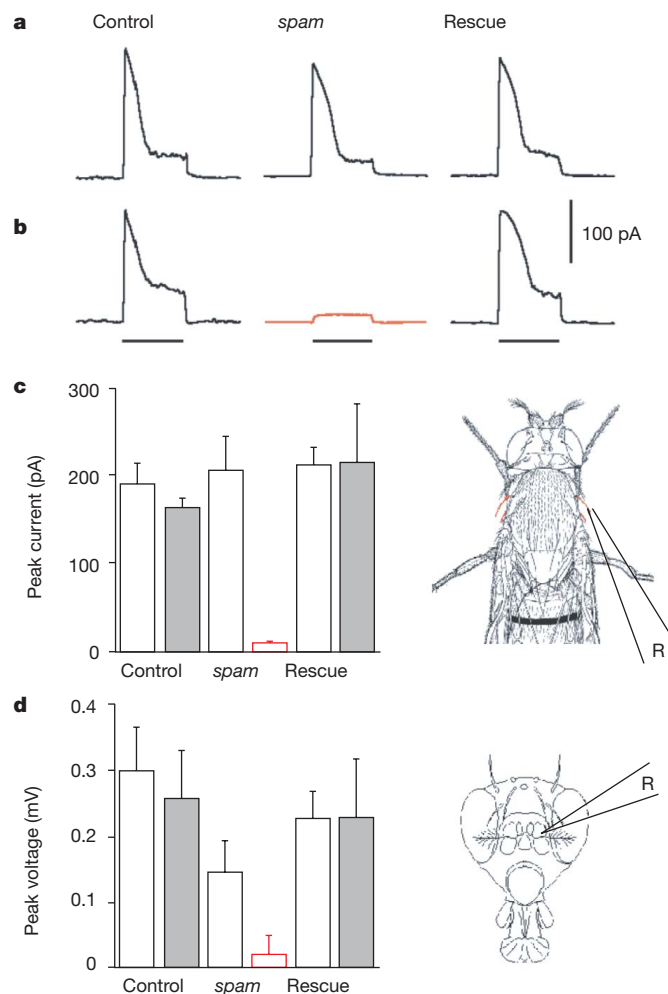


Figure 1 | Effect of heat exposure on the function of mechanoreceptor cells. **a, b**, MRN responses from a single voltage-clamped bristle to mechanical stimuli. **a**, (left to right): responses of control (*cn bw* flies), *spam* (*spam/spam* mutants) and rescue flies (*spam* homozygotes expressing a wild-type *spam* transgene). Note normal responses of all three samples at 21 °C. **b**, After incubation for 30 min at 37 °C, responses were abolished in *spam* mutants (red trace). Lines under the traces indicate the duration of 0.3 s of a deflection stimulus of 30 μ m. **c**, Summary of peak responses of **a, b** (right-hand diagram illustrates the site of recordings). **d**, Summary of peak extracellular voltage responses to antennal rotation (pipette position illustrated on the right-hand diagram). Open columns, 21 °C; hatched columns, responses after 30 min at 37 °C. R, the position of the recording pipette. Error bars, s.d. ($n \geq 6$ for each trial).

¹Howard Hughes Medical Institute and Departments of Neurobiology and Neurosciences, University of California at San Diego, La Jolla, California 92093-0649, USA. ²Department of Biochemistry and Molecular Biophysics, Washington University School of Medicine, St Louis, Missouri 63110, USA.

directly examine the impact of loss-of-function mutations in *spam* on mechanosensory transduction, we performed electrophysiological recordings from bristle mechanoreceptors (touch)⁹ and antennal chordotonal organs (hearing)¹⁰ from control and mutant flies. We gave sensory bristles calibrated mechanical stimuli while recording transduction currents with a voltage-clamp apparatus. At 21 °C, control flies and *spam* mutants displayed robust inward currents in response to bristle deflections (Fig. 1a–c). In contrast, 30 min of exposure to 37 °C reduced mechanoreceptor response amplitudes in *spam* mutant animals by over 80%. The same heat exposure also nearly abolished all mechanoreceptor antennal responses, while having no significant effect on control flies (Fig. 1d).

Next, we examined the ultrastructure of MRNs in control flies and *spam* mutants at both permissive and non-permissive temperatures. *Drosophila* mechano- and chemosensory neurons house their entire sensory apparatus in a ciliated outer segment that forms the neuronal sensory endings¹¹. In MRNs, this outer segment is bathed in an extracellular fluid (lymph) which provides the proper ionic environment for the generation of mechanoreceptor currents¹¹. Remarkably, *spam* mutants, but not control flies, experience a dramatic deformation of their MRNs in response to heat treatment: the entire neuronal cytoplasm invades the lymph space, such that the region that normally

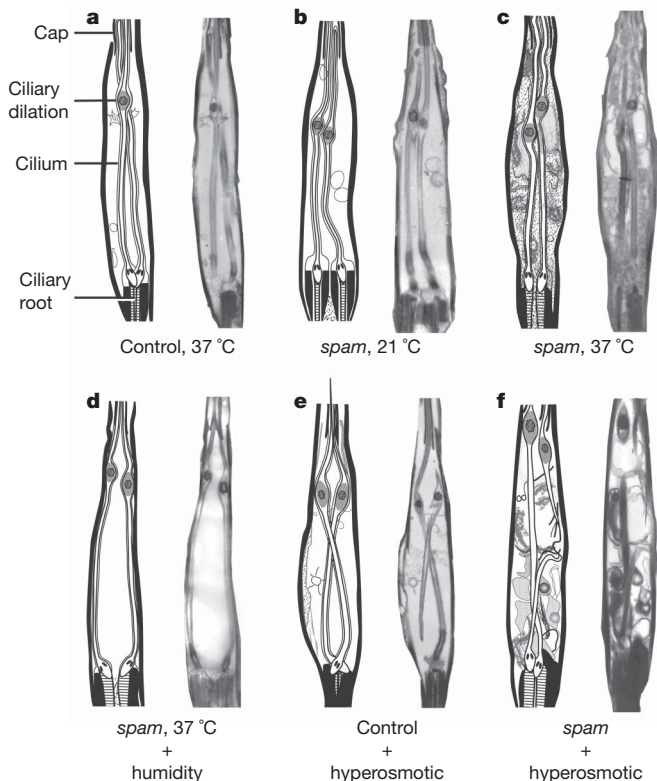


Figure 2 | Mechanoreceptors of *spam* mutants undergo dramatic cellular deformation. Electron micrographs of a typical scolopale MRN in the Johnston's organ. **a**, Control (*cn bw*) flies at 37 °C and **(b)** *spam* homozygous mutants at 21 °C have nearly indistinguishable morphology (equivalent results are observed with *cn bw* flies at 21 °C). However, **(c)** exposure of *spam* flies to 30 min at 37 °C results in major cellular deformation, with the receptor cell cytoplasm expanding to fill the entire scolopale space (importantly, the cells that wrap around the scolopale space are unaffected; data not shown). **d**, Placing *spam* mutants in a high-humidity chamber (greater than 90% relative humidity) prevents the heat-induced deformation. **e, f**, *cn bw* control and *spam* flies injected with a hyper-osmotic solution to the abdomen. Only *spam* mutants display dramatic cellular deformation with extensive invasion of the extracellular space. Note that some of the reconstructed electron micrographs show a side view of the scolopale, with only one ciliary root visible (**a** and **e**), whereas all others show a front view, with both ciliary roots visible.

contained only the cilium and extracellular fluid now becomes filled with cellular material from the MRN cell body (compare Fig. 2a, b and Fig. 2c; see also Supplementary Figs 2 and 4).

How does exposure to elevated temperatures have such a dramatic effect on the morphology of *spam* MRNs? Changes in molecular thermal motion between 21 °C and 37 °C are too small, and unlikely to account for the phenotype. We therefore considered a prominent secondary effect of heat: water loss by evaporation. To investigate how much water is lost during the heat exposure, we measured the weight of control and mutant flies at intervals of 15 min. All flies lose about 20% of their total weight after 60 min at 37 °C (about 25% of their water content; data not shown), yet only the mutants display the mechanosensory defect. To determine whether the heat-induced deformation of MRN in *spam* mutants is indeed a consequence of water loss, we placed *spam* flies either in a control Petri dish or in a dish at over 90% humidity, and subjected them to 37 °C for 60 min. Notably, only the flies in the dry chamber were affected by heat; exposure to high humidity during the high-temperature treatment completely prevented the manifestation of the mutant phenotype, both morphologically (Fig. 2c, d) and behaviourally (Supplementary material, compare Supplementary Videos 4 and 6). These data demonstrate that the mutant's mechanosensory deficit does not arise from an effect of temperature per se, but is instead triggered by excessive water evaporation at high temperature¹². Why does water loss lead to deformation of the MRN only in *spam* mutants? We hypothesized that the rapid loss of water from the animal's circulatory system (haemolymph) would increase its osmolarity, leading to an outflow of water from the sensory lymph. The new imbalance between the MRN cytoplasm and the lymph would cause the deformation of the MRN cytosol, which if not contained (as in the absence of Spam protein; see below), would then invade the lymph space. This proposed mechanism anticipates that hypertonic shock to the haemolymph of *spam* mutants, but not wild-type animals, should mimic the effect of high temperature on the morphology and function of MRNs (that is, hypertonic shock should induce a similar osmotic imbalance between the endolymph and the cytoplasm of the MRN). We injected a high-osmolarity solution to the abdomen of *spam* and control flies and prepared them for examination by electron microscopy. As hypothesized, only *spam* flies showed deformation of the MRN (Fig. 2e, f) and loss of mechanosensory responses (Supplementary Fig. 3), substantiating the mechanism of deformation and the role of Spam in maintaining cell shape.

In photoreceptor neurons, Spam is secreted into the inter-rhabdomeral space, where it forms the extracellular medium that organizes and preserves the separation of rhabdomeres. We reasoned that in mechanoreceptor neurons the role of Spam might be a variation on this theme, perhaps serving as a cellular exoskeleton that provides structural rigidity to the MRN, thus ensuring the preservation of cell shape under environmental stress. This postulate makes two significant predictions. First, Spam protein should be specifically localized within the fly's mechanoreceptor organ, at locations that might be particularly vulnerable to osmotic pressure changes. Second, if Spam functions as a mechanical barrier that protects MRN from deformation, it should be possible to engineer cells that are coated with Spam and make them resistant to osmotic insult and deformation pressures. Indeed, Spam protein concentrates at two specific sites in MRN: one, right at the interface between the MRN cell body and the lymph space, the very domain that collapses at high temperature in mutant animals (see Supplementary Fig. 4d, e); and at a second site close to the ciliary dilation, possibly helping sustain the two ciliary processes at the proper position (Supplementary Fig. 4). To generate cells that are decorated by a layer of Spam, we took advantage of Spam's ability to directly bind the membrane receptor Prolaminin⁷. Therefore, *Drosophila* tissue culture cells expressing and secreting Spam were incubated with GFP-labelled cells transfected with Prolaminin. As expected, secreted Spam specifically decorated the surface of Prolaminin-expressing cells; to identify those

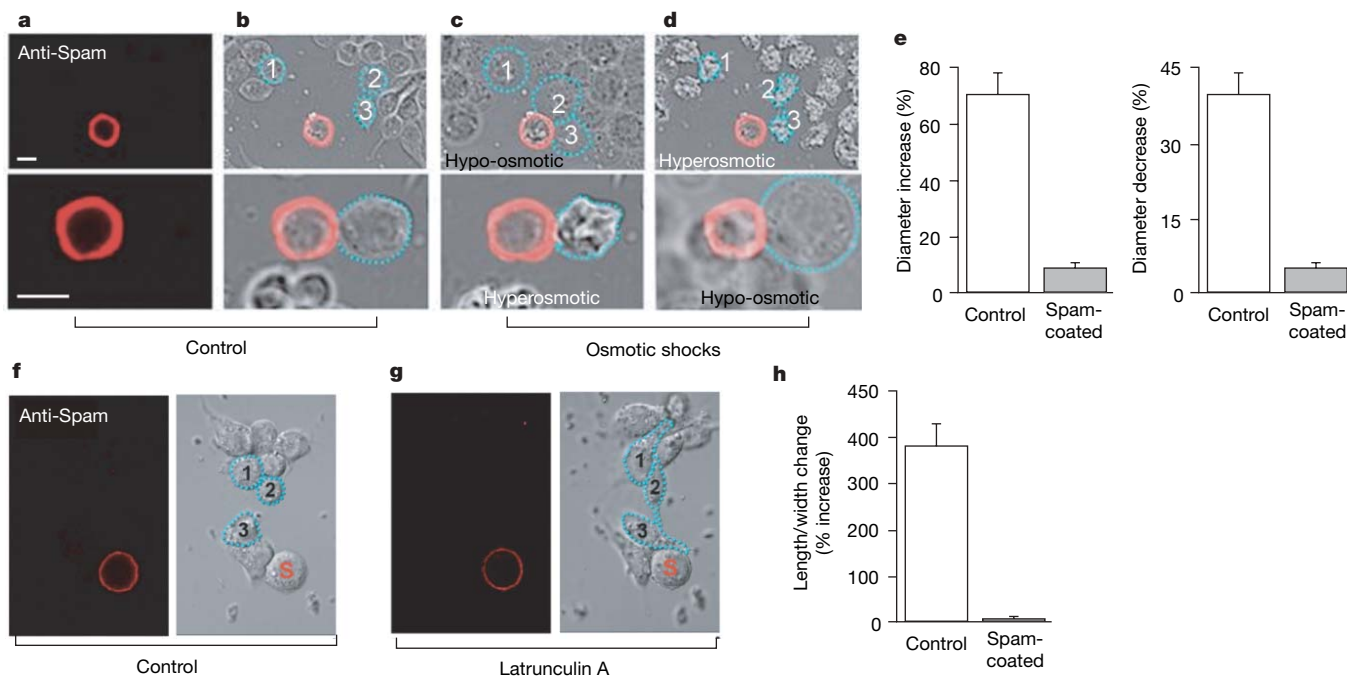


Figure 3 | Spam coating prevents cell deformation induced by osmotic or chemical manipulation. **a–d**, Kc tissue culture cells transfected with Prom and Spam were stained for Spam surface labelling (red) using anti-Spam antibodies on unpermeabilized, intact cells. Spam-coated (**a**) and uncoated cells were then subjected to osmotic shock. **b–d**, Upper panels show low-magnification images of cells before and after sequential hypo- and hyper-osmotic shock; lower panels show similar cells at higher magnification but this time after sequential hyper- and then hypo-osmotic shock (reverse order). Hypo-osmotic shock causes dramatic swelling of uncoated cells, whereas hyper-osmotic treatment of the same preparation leads to extreme shrinking. Notably, the Spam-coated cell remains largely unaffected by both treatments. All cells that showed a continuous layer of Spam coating (a layer thicker than $0.5\ \mu\text{m}$ with no apparent gaps) showed no significant shape

changes in response to the osmotic shocks ($n = 11$), whereas all uncoated cells displayed severe changes in size and shape ($n > 150$). **e**, Increases (left) and decreases (right) in cell size after hypotonic or hypertonic shock; control, $n \geq 24$; spam-coated, $n \geq 8$; error bars, s.e.m. **f**, Spam-coated (red) and uncoated cells were incubated for 90 min with latrunculin A. **g**, As expected, control cells undergo dramatic changes in cell shape¹³. In contrast, the spam-coated cell (S) remains unaltered. Blue dots and numbers delineate the shape of three sample uncoated cells before (**f**) and after (**g**) treatment. Images were captured with epifluorescence and Nomarski interference contrast. **h**, Changes in cell shape (defined as changes in the ratio of cell length over width) after treatment with latrunculin in Spam-coated ($n = 9$) and control uncoated cells ($n = 27$); error bars, s.e.m.

cells that are entirely (or nearly completely) coated, we performed immunofluorescent staining with anti-Spam antibodies. We induced cellular deformation by subjecting control and coated cells to hyper- and hypo-osmotic solutions. As predicted, control cells undergo significant swelling after hypo-osmotic shock, and severe shrinking in the presence of hyper-osmotic solutions (Fig. 3a–e). In contrast, coated

cells were largely resistant to these treatments and showed only minor changes in shape and size (not surprisingly, poorly coated cells were indistinguishable from controls; data not shown). Next, we examined the impact of Spam on chemically induced changes in cell shape¹³. We subjected control cells to latrunculin A and elicited dramatic changes in cell morphology (Fig. 3f–h). However, Spam-coated cells retained their normal spherical shape, even after extensive actin remodelling resulting from the treatment with latrunculin A (see Methods). Collectively, these studies demonstrate that Spam coating of the plasma membrane endows cells with exquisite protection against osmotically and chemically induced transformations in cell shape.

How robust are Spam-treated cells? We directly examined the stiffness of Spam-coated and control cells by measuring their mechanical properties. In these experiments, a glass filament of known bending constant is continuously pressed against the cell by a linear piezoelectric drive¹⁴ (Fig. 4a, b). The force applied to the tip of the probe by the resistance of the cell to indentation is then calculated by optically measuring the bending of the glass probe. The major source of stiffness in cells is the actin cytoskeleton¹⁵. Therefore, to eliminate the contribution of the cytoskeleton and explore the specific effect of Spam, experimental and control samples were first treated with cytochalasin D for 120 min. The results (Fig. 4c) demonstrate that Spam-coated cells exhibit stiffness that is approximately ten times that of control cells.

Together, these studies have revealed a remarkable solution to the problem of maintaining cellular integrity and structure under duress. They also provide a salient example of evolution using the same protein to satisfy two very different needs: the building of compound eyes in open rhabdom systems^{7,16}, and the preservation of cell shape

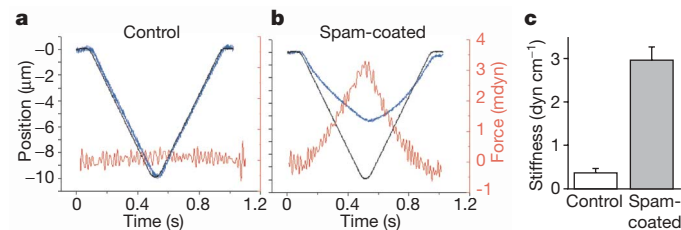


Figure 4 | Mechanical impact of Spam coating. To measure the stiffness of Spam-coated cells, (**a**) control or (**b**) Spam-coated tissue culture cells were subjected to a mechanical indentation assay¹⁴. To reduce the contribution of the cytoskeleton to cell stiffness (and thereby reveal the effect of Spam coating more effectively), samples were pre-treated with cytochalasin D as previously described¹⁵. **a**, **b**, Comparison of the position over time of the motor that moves the probe assembly (black trace) versus the position of the stylus that indents the cell (blue trace). The difference between the two curves at a given time is due to the cell's resistance to indentation. The force applied by the cell against the probe is proportional to this difference and is shown in red. **c**, Stiffness (cell resistance force per unit indentation) was calculated as described¹⁴. A minimum of nine individual cells were examined for each experiment; error bars, s.e.m. Control cells without cytochalasin D are presented in Supplementary Fig. 5.

in mechano- and chemoreceptor organs. Interestingly, both entail the production and assemblage of a rigid substrate, thus highlighting the fundamental role of Spam in tissue morphogenesis (in one scenario to ensure the partitioning and maintenance of the rhabdomere complex, and in the other to guarantee the mechanical integrity of sensory neurons). Finally, it is worth noting that the ability to assemble a 'cell wall' surrounding an animal cell may provide the foundation for important applications in cell engineering, where resistance to osmotic pressures may be warranted, or where preservation of cell and tissue structure (or tone) may be needed.

METHODS SUMMARY

Fly stocks. An isogenized *cn bw* stock was used as control in all experiments. The *spam* line was isolated from the Zuker collection⁶ and the rescue was done using *hs-gal4* driving *UAS-spam*⁷.

Electrophysiology. Single bristle current recordings were performed as described earlier⁹. Voltage changes resulting from activation of Johnston's organ were monitored by inserting a glass pipette (2 M KCl, approximately 10 M Ω) into the second antennal segment. Mechanical stimulation was delivered by a stream of air that was directed at the arista, causing a rotation of the third segment for the duration of air flow.

In vivo osmotic manipulation. Flies were glued ventral side up and manually injected by using a glass pipette with a tip of 20–40 μ m. After 10 min, tissue was prepared for analysis as described under Electron microscopy.

Electron microscopy. Heads of 7- to 10-day-old flies were fixed and sectioned exactly as previously described⁷. A series of coronal sections (100–200 nm per section) through the antennal second segment was obtained. The entire scolopale was reconstructed from overlapping sections using Adobe imaging software.

Tissue culture. Kc cells¹³ were transfected with combinations of pTub-GAL4 and pUAST-spacemaker, pUAST-prominin and pUAST-GFP, as previously described⁷. Spam coating was detected *in vivo* by using its specific antibody mAb21A6¹⁷. Hypo-osmotic shock was induced by diluting the growth medium 1:5 \times with distilled water; hyper-osmotic conditions were obtained by adding 50 μ l of 5 M NaCl to 1.25 ml of growth media. Latrunculin A (Sigma) was used at a final concentration of 0.2 μ M (ref. 18).

Cell indentation assay. KC cells co-transfected with pTub-GAL4, pUAST-spacemaker and pUAST-prominin were treated with 2 μ M cytochalasin D for at least 100 min, and the Spam-coated cells identified by labelling with anti-Spam antibodies. Indentation tests were performed on control and Spam-coated cells as previously described¹⁴.

Full Methods and any associated references are available in the online version of the paper at www.nature.com/nature.

Received 3 September; accepted 20 December 2007.

Published online 24 February 2008.

- Colclasure, J. C. & Holt, J. R. Transduction and adaptation in sensory hair cells of the mammalian vestibular system. *Gravit. Space Biol. Bull.* **16**, 61–70 (2003).
- Hudspeth, A. J. How the ear's works work. *Nature* **341**, 397–404 (1989).

- Barth, F. G. Spider mechanoreceptors. *Curr. Opin. Neurobiol.* **14**, 415–422 (2004).
- Kernan, M., Cowan, D. & Zuker, C. Genetic dissection of mechanosensory transduction: mechanoreception-defective mutations of *Drosophila*. *Neuron* **12**, 1195–1206 (1994).
- Kernan, M. & Zuker, C. Genetic approaches to mechanosensory transduction. *Curr. Opin. Neurobiol.* **5**, 443–448 (1995).
- Koundakjian, E. J., Cowan, D. M., Hardy, R. W. & Becker, A. H. The Zuker collection: a resource for the analysis of autosomal gene function in *Drosophila melanogaster*. *Genetics* **167**, 203–206 (2004).
- Zelhof, A. C., Hardy, R. W., Becker, A. & Zuker, C. S. Transforming the architecture of compound eyes. *Nature* **443**, 696–699 (2006).
- Husain, N. *et al.* The agrin/perlecan-related protein eyes shut is essential for epithelial lumen formation in the *Drosophila* retina. *Dev. Cell* **11**, 483–493 (2006).
- Walker, R. G., Willingham, A. T. & Zuker, C. S. A *Drosophila* mechanosensory transduction channel. *Science* **287**, 2229–2234 (2000).
- Gopfert, M. C. & Robert, D. Biomechanics. Turning the key on *Drosophila* audition. *Nature* **411**, 908 (2001).
- Keil, T. A. Functional morphology of insect mechanoreceptors. *Microsc. Res. Tech.* **39**, 506–531 (1997).
- Gibbs, A. G., Louie, A. K. & Ayala, J. A. Effects of temperature on cuticular lipids and water balance in a desert *Drosophila*: is thermal acclimation beneficial? *J. Exp. Biol.* **201**, 71–80 (1998).
- Kiger, A. A. *et al.* A functional genomic analysis of cell morphology using RNA interference. *J. Biol.* **2**, (<http://jbiol.com/content/pdf/1475-4924-2-27.pdf>) (2003).
- Zahalak, G. I., McConnaughey, W. B. & Elson, E. L. Determination of cellular mechanical properties by cell poking, with an application to leukocytes. *J. Biomech. Eng.* **112**, 283–294 (1990).
- Wakatsuki, T., Schwab, B., Thompson, N. C. & Elson, E. L. Effects of cytochalasin D and latrunculin B on mechanical properties of cells. *J. Cell Sci.* **114**, 1025–1036 (2001).
- Osorio, D. Spam and the evolution of the fly's eye. *Bioessays* **29**, 111–115 (2007).
- Zipursky, S. L., Venkatesh, T. R., Teplow, D. B. & Benzer, S. Neuronal development in the *Drosophila* retina: monoclonal antibodies as molecular probes. *Cell* **36**, 15–26 (1984).
- Spector, I., Shochet, N. R., Blasberger, D. & Kashman, Y. Latrunculins – novel marine macrolides that disrupt microfilament organization and affect cell growth. I. Comparison with cytochalasin D. *Cell Motil Cytoskeleton* **13**, 127–144 (1989).

Supplementary Information is linked to the online version of the paper at www.nature.com/nature.

Acknowledgements We particularly thank E. L. Elson for his help and hospitality in the cell poking studies. We are also indebted to A. Zelhof for advice, materials and reagents, and T. Avidor-Reiss for his help with the immunolocalization of Spam. We thank T. Meerloo for help with immunogold labelling, and A. Becker for help with tissue culture and transfections. We thank N. Ryba, A. Kiger and members of the Zuker laboratory for comments. C.S.Z. is an investigator of the Howard Hughes Medical Institute.

Author Information Reprints and permissions information is available at www.nature.com/reprints. Correspondence and requests for materials should be addressed to C.S.Z. (charles@flyeye.ucsd.edu).

METHODS

Fly stocks. An isogenized *cn bw* stock was used as control in all experiments. The *spam* line was isolated from the Zuker collection⁶ and the rescue was done using *hs-gal4* driving UAS-*spam*⁷.

Electrophysiology. Single bristle current recordings were performed as described earlier⁷. Voltage changes resulting from activation of Johnston's organ were monitored by inserting a glass pipette (2 M KCl, approximately 10 M Ω) into the second antennal segment. Mechanical stimulation was delivered by a stream of air that was directed at the arista, causing a rotation of the third segment for the duration of air flow. Signals were acquired with an EX1 differential amplifier (DAGAN) and a pCLAMP (Axon Instruments) system, and analysed with Origin (Microcal Software).

In vivo osmotic manipulation. Flies were glued ventral side up and manually injected by using a glass pipette with a tip of 20–40 μm . A volume of 0.2 μl of a solution containing 1 M mannitol was injected into the abdomens of male and female control or *spam* mutant flies. After 10 min, tissue was prepared for analysis as described under Electron microscopy.

Electron microscopy. Heads of 7- to 10-day-old flies were fixed and sectioned exactly as previously described⁷. A series of coronal sections (100–200 nm per section) through the antennal second segment was obtained and examined with a JEOL 1200EX II or a Philips CM-10 transmission electron microscope; at least three flies from a minimum of two independent experiments were examined. The entire scolopale was reconstructed from overlapping sections using Adobe imaging software.

Tissue culture. To coat cells with a layer of Spam, we took advantage of its selective binding to Prominin, the Spam receptor in photoreceptor cells⁷. The nature of the Spam receptor in MRNs, if any, is not yet known. Kc cells¹³ were transfected with combinations of pTub-GAL4 and pUAST-spacemaker, pUAST-prominin and pUAST-GFP, as previously described⁷. Spam coating was detected *in vivo* by incubation for 45 min with mAb21A6¹⁷ (1:100 in growth medium), followed by incubation for 45 min with Red-x-conjugated secondary antibody (Jackson ImmunoResearch Laboratories). Hypo-osmotic shock was induced by diluting the growth medium 1:5 \times with distilled water; hyper-osmotic conditions were obtained by adding 50 μl of 5 M NaCl to 1.25 ml of growth media. Vital staining was performed by addition of Trypan blue (0.04% final concentration, GIBCO) to the growth medium. Latrunculin A (Sigma) was used at a final concentration of 0.2 μM (ref. 18) to prevent polymerization of actin. To ensure that latrunculin A was effective in disrupting actin cytoarchitecture, control and Spam-coated cells were labelled with fluorescein isothiocyanate (FITC)-conjugated phalloidin (Invitrogen). In all cases, latrunculin A induced the formation of F-actin aggregates (data not shown). Time-lapse imaging of transmitted and fluorescent signals was performed by using either a BioRad MRC1024 or an Olympus FluoView1000 confocal microscope. Changes in cell size in the hypotonic shock studies were analysed by measuring the cell's diameter before and after osmotic shock. Changes in cell shape in the latrunculin experiments were quantified by using the ratio between the cell's length (defined as its longest axis) and its width (perpendicular to the length) before and after drug treatment. Cells were measured by standard imaging software, and data analysed by Origin Software.

Cell indentation assay. Kc cells co-transfected with pTub-GAL4, pUAST-spacemaker and pUAST-Prominin were treated with 2 μM cytochalasin D for at least 100 min (to interrupt F-actin formation by capping the barbed ends), and the Spam-coated cells identified by labelling with anti-spam antibodies. Indentation tests were performed on control and Spam-coated cells as previously described¹⁴ by using a probe with a spring constant of 6.72 dyne cm^{-1} and a tip diameter of 5 μm . Data were analysed exactly as described previously, with stiffness (K) defined as $K = G[1 - (dM/dt)/(dP/dt)]$, where $M(t)$ is motor position, $P(t)$ is tip position and G is probe stiffness; this calculation does not take into account inertia and viscous drag¹⁴. Probe control, data collection and analysis were performed with the Experix environment (<https://sourceforge.net/projects/experix>).